molecules

MDPI

Article

Synthesis and Characterization of Nano-Conducting Copolymer Composites: Efficient Sorbents for Organic Pollutants

Khadija M. Emran [1], Shimaa M. Ali [1,2,*] and Aishah L. L. Al-Oufi [1]

[1] Department of Chemistry, Faculty of Science, Taibah University, Madinah 30002, Saudi Arabia; k_and_e154@hotmail.com (K.M.E.); aloosh200933@hotmail.com (A.L.L.A.-O.)

[2] Department of Chemistry, Faculty of Science, Cairo University, Giza 12613, Egypt

* Correspondence: dr_shimaaali80@yahoo.com; Tel.: +966-556-793-098

Academic Editor: Kei Saito

Received: 10 March 2017; Accepted: 5 May 2017; Published: 10 May 2017

Abstract: Nano-conducting copolymers of aniline (ANI) and pyrrole (Py) with silica of different starting monomer ratios are prepared by oxidative chemical polymerization. X-ray diffraction (XRD) data showed that polyaniline (PANI) is the predominant phase in copolymer composites with a higher starting ANI monomer ratio while polypyrrole (PPy) is the major phase for other prepared samples. Transmission and scanning electron microscope images ascertained XRD results where hexagonal-shaped particles are assigned to PANI/SiO_2 and poly(9ANI-co-1Py)/SiO_2 samples; the cauliflower morphology can be observed for PPy/SiO_2, poly(1ANI-co-9Py)/SiO_2, poly(1ANI-co-2Py)/SiO_2, and poly(1ANI-co-1Py)/SiO_2 samples. One-dimensional nano-fibers can be obtained by using a starting monomer ratio of 2ANI:1Py during synthesis. Thermal analysis showed that copolymerization increases the thermal stability as compared with PANI/SiO_2 and PPy/SiO_2 composites. All prepared samples were applied as sorbents for Congo red dye from aqueous solutions. It was found that the sorption capacity value was affected by the starting monomer ratio; poly(2ANI-co-1Py)/SiO_2 has the highest sorption capacity; the q_m value is 142.9 mg g^{-1} due to its highly-stabilized nano-structure.

Keywords: nano-composite; copolymerization; characterization; adsorption; organic dye

1. Introduction

Conducting polymers, such as polypyrrole (PPy), polythiophene (PT), polyaniline (PANI), polyfuran (PF), and derivatives, are conjugated π-electron systems that promote the charge-transfer process due to their considerable electrical conductivity and they offer many other interesting properties—thermal, optical, mechanical, etc.—that make them promising candidates for many scientific researches and applications [1]. Conducting polymer composites can be formed by introducing a secondary organic/inorganic component so that enhanced properties—compared to individual components—can be obtained by a combined interaction between the organic/inorganic component and the host polymer matrix [2]. Copolymerization can be used to modify physical properties and overcome drawbacks of individual polymers. Several conducting copolymer composites showed improved properties in many applications. Nano-structured copolymer of aniline (ANI) and pyrrole (Py), (poly(ANI-co-Py)), synthesized at low temperature showed enhanced and selective ammonia sensing behavior as compared with individual polymers PANI and PPy [3]. Zeolite-based nickel-deposited poly(Py-co-fluoro-ANI)/CuS [4] and nano-sulfur/poly(Py-co-ANI) [5] were used as efficient catalysts in sulfur fuel cell applications. Poly(ANI-co-Py)/graphene oxide [6] and transition metal doped poly(ANI-co-Py)/multi-walled carbon nanotube nanocomposite [7] were employed as

high performance supercapacitor electrode materials. Zinc-modified poly(ANI-co-Py) coatings showed excellent anti-corrosive performance on low nickel stainless steel [8]. Interconnected poly(ANI-co-Py) nanofibers showed efficient removal of organic pollutants such as Congo red (CR) dye [9], as well as inorganic contaminants such as Cr(IV) ions [10] from aqueous solutions by adsorption.

Congo red, a benzidine-based anionic diazo-dye, constitutes a major common component in colored wastewater resulted from many textile industries [11]. The removal of such pollutants is very important as their presence causes harmful effects to the environment and to humans. Various methods can be employed in the discharging process such as chemical oxidation, electrochemical method, coagulation, ion exchange, and adsorption. Among these methods, adsorption offers the advantages of simplicity, effectiveness, and low cost [12]. Several materials were reported in literature as sorbents for organic dyes [13–18], such as conducting polymers [19,20] which are non-toxic, stable under many environmental conditions, can be synthesized in large scale and contain functional groups that promote them as efficient sorbents. Various PANI [21–31], PPy [32–35], and poly(ANI-co-Py) [9] nano-composites are employed for the removal of organic dyes from aqueous solutions. However, the effect of the starting monomer ratio on the sorption properties has not yet been discussed.

In this work, nano-conducting copolymer composites are prepared by the chemical oxidation of two monomers, ANI and Py, with ferric chloride oxidant in the presence of SiO_2 nano-paticles and CTAB surfactant. The effect of the starting monomer ratio on structural, surface, and thermal properties is investigated and compared with those properties of individual polymer composites. Prepared nano-conducting polymer composites are applied for the first time for the removal of Congo red from aqueous solutions by adsorption. A proper adsorption isotherm is presented and maximum adsorption capacity values are calculated. These values are discussed and elucidated based on the starting monomer ratio effect on the composite characterizations. In our previous study [36], the effect of the nano-inorganic oxide type in the composite on its sorption capacity for CR has been examined. It is found that nano-silica/PANI composite has a moderate sorption capacity, so it has been chosen in this study to show the enhancement caused by the copolymerization.

2. Results and Discussion

2.1. Characterizations of Nano-Copolymer Composites

2.1.1. X-ray Diffraction Structural Characterization

Figure 1 shows X-ray Diffraction (XRD) patterns of homo-PANI and PPy composites with SiO_2 together with its copolymer composites with SiO_2. Poly(ANI-co-Py) composites are prepared in different monomer ratios: 1:1, 1:2, 2:1, 1:9, and 9:1.

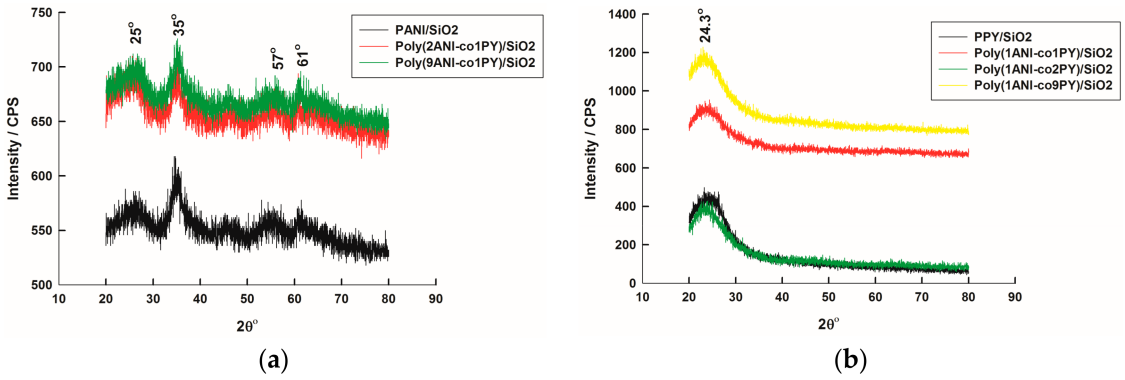

Figure 1. X-ray diffraction (XRD) spectra of homo-polyaniline (PANI), polypyrrole (PPy) and different copolymer of aniline (ANI) and pyrrole (Py) (poly(ANI-co-Py)) composites with SiO_2; peaks of PANI (**a**) and PPy (**b**) are indexed.

Table 1 summarizes 2θ values of constituting components of homo- and copolymer composites, SiO_2, PANI, and PPy. It can be observed that a broad peak appears at around 2θ = 26° [37], for all samples, with an intensity lower than 100 which ascertains the presence of hexagonal amorphous SiO_2 in all composites as a secondary phase. PANI constitutes the major phase in homopolymer composite with SiO_2, PANI/SiO_2, and in poly(2ANI-co-1Py)/SiO_2 and poly(9ANI-co-1Py)/SiO_2 samples since its major peak, at 2θ value of 35°, has an intensity value of 100 [38,39], as shown in Figure 1a. On the other hand, PPy is the major phase in homopolymer composite with SiO_2, PPy/SiO_2, and in poly(1ANI-co-1Py)/SiO_2, poly(1ANI-co-2Py)/SiO_2, and poly(1ANI-co-9Py)/SiO_2 samples since the major peak (intensity of 100) belongs to PPy at 2θ value of 24.3°, as shown in Figure 1b. It was reported previously that the XRD spectrum of the amorphous PPy has a characteristic single broad peak at around 2θ value of 25° [40]. This slight change in 2θ value may be due to the formation of a composite with SiO_2 [41].

It can be observed that all copolymer composites have higher peak intensities than those of homopolymer composite which indicates the increase in crystallinity of composites upon copolymerization. In addition, in all copolymer composite samples, two polymers, PANI and PPy, exist. However, in poly(2ANI-co-1Py)/SiO_2 and poly(1ANI-co-2Py)/SiO_2, only one polymer phase is present which is PANI or PPy, respectively; this suggests the formation of a copolymer phase in which the absent polymer component cannot be identified (random or branched copolymers).

The Brunauer, Emmett, and Teller (BET) surface area values of all prepared samples, homo- and copolymer composites, are listed in Table 1. It can be seen that the copolymerization decreases the surface area values as compared with the surface area values of individual polymer composites, PANI/SiO_2 and PPy/SiO_2. This reduction is more pronounced for comparable starting monomer ratios, i.e., using the starting (1:1) monomer ratio in the synthesis results in the copolymer composite with the lowest surface area, followed by the 1:2 ratio and finally the 1:9 ratio results in the largest surface area; however, in all cases, the surface area is still smaller than that of homopolymer composites. A possible reason for the reduction in surface area values is the core-shell structure, with silica core, that results in a larger particle size and in turn a lower surface area.

2.1.2. Surface Characterizations by Transmission and Scanning Electron Microscopes

Transmission electron microscope (TEM) images of PANI, PPy, and different copolymer composites with SiO_2 are shown in Figure 2a–g. The morphology of PPy/SiO_2 composite has a characteristic cauliflower shape, Figure 2a. Similar morphology can be shown by poly(1ANI-co-9Py)/SiO_2, poly(1ANI-co-2Py)/SiO_2, and poly(1ANI-co-1Py)/SiO_2 samples, as shown in Figure 2c,e,g, respectively. This agrees with XRD results, where the major constituting phase in these samples is PPy. On the other hand, hexagonal-shaped particles of PANI/SiO_2 composite can be clearly shown in Figure 2b,d, assigned to the poly(9ANI-co-1Py)/SiO_2 sample. It can be observed that the poly(2ANI-co-1Py)/SiO_2 sample, Figure 2f, consists of unique needle-shaped, 1D nano-fiber particles, instead of the expected hexagonal-shaped particles. The preparation of PANI nano-fibers has been successively done by Kaner et al. [42], through the conventional chemical oxidative polymerization of ANI. It was reported that the use of PANI nano-fibers or their composites can significantly enhance the catalytic and sensing properties due to the self-stabilization of nano-fibers by electrostatic repulsions. As a conclusion, it is possible to control the morphology of the copolymer composite by changing the starting monomer ratio.

Table 1. 2θ, peak intensity values and Brunauer, Emmett, and Teller (BET) surface areas of constituting homo-polyaniline (PANI), polypyrrole (PPy) and copolymers, (poly(ANI-co-Py)) with different starting monomers ratios, composites with SiO_2 [36].

		PANI/SiO_2 Sample		**PPy/SiO_2 Sample**		**Poly(1ANIco1Py)/SiO_2 Sample**		**Poly(1ANIco2Py)/SiO_2 Sample**		**Poly(2ANIco1Py)/SiO_2 Sample**		**Poly(1ANIco9Py)/SiO_2 Sample**		**Poly(9ANIco1Py)/SiO_2 Sample**	
Standard SiO_2															
2θ	I	2θ	I	2θ	I	2θ	I	2θ	I	2θ	I	2θ	I	2θ	I
20	20	20.4	24	-	-	-	-	-	-	-	-	-	-	-	-
26	100	26.0	24	26.0	95	26.1	76	26.1	65	26.1	79	26.3	63	26.0	45
Standard PANI															
25	45	25.1	28	-	-	-	-	-	-			-	-	-	-
35	100	35.0	100	-	-	35.2	18	No Peak		34.9	100	34.8	7	35.1	100
57	21	57.0	16	-	-	-	-	-	-			-	-	57.1	14
61	24	60.7	36	-	-	-	-	-	-	60.9	53	-	-	61.0	43
Standard PPy															
24.3	100	-	-	24.3	100	24.1	100	24.1	100	No peak		24.3	100	24.5	35
BET surface area/$m^2\ g^{-1}$		72.40		122.81		24.23		47.99		53.69		55.01		68.43	

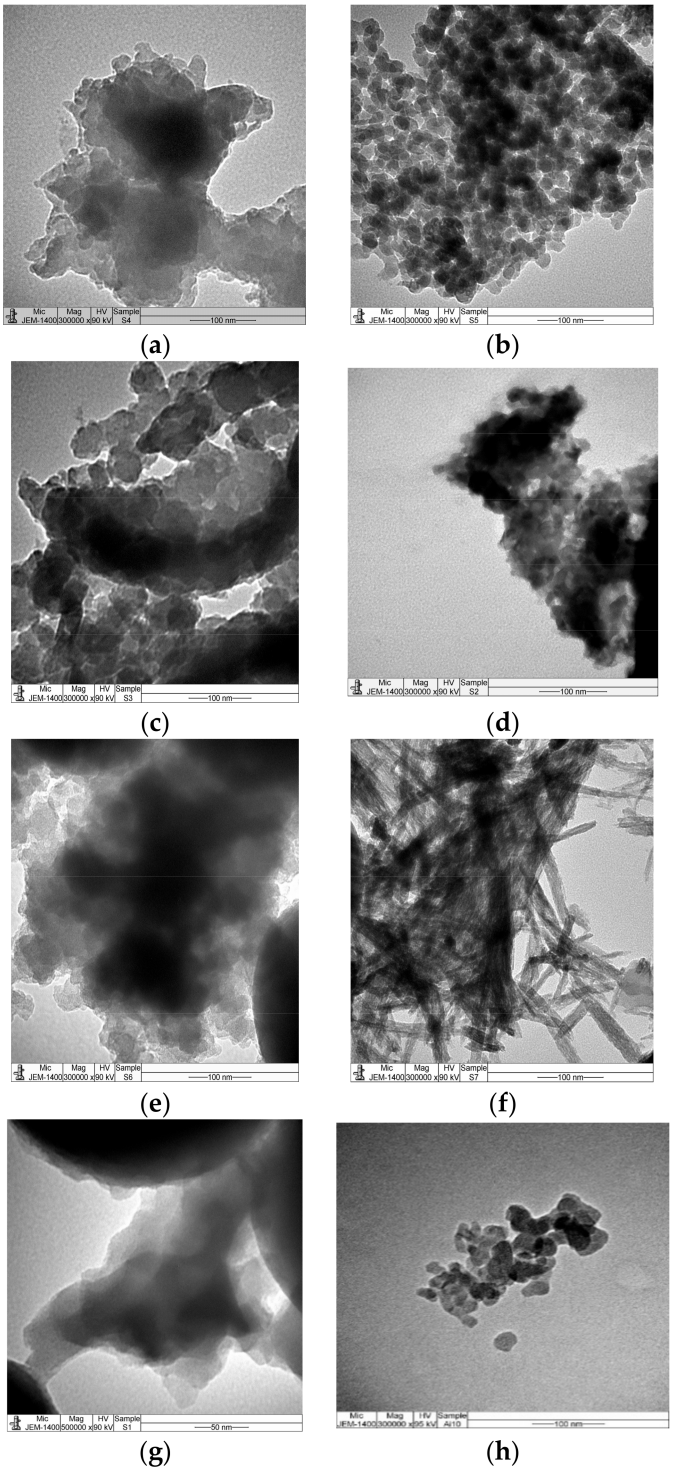

Figure 2. Transmission electron microscopy (TEM) images of PPy/SiO_2 (**a**); PANI/SiO_2 (**b**), and different poly(ANI-co-Py) composites in the monomer ratios of 1:9 (**c**); 9:1 (**d**); 1:2 (**e**); 2:1 (**f**); 1:1 (**g**); and silica (**h**).

Scanning electron microscope (SEM) photos for PANI, PPy, and different copolymer composites with SiO_2 are shown in Figure 3. For PPy/SiO_2 composite, the compact cauliflower morphology can be seen, while in case of silica phase, it cannot be identified from the SEM image, as shown in Figure 3a. The same morphology is assigned to the poly(1ANI-co-9Py)/SiO_2 sample, as shown in Figure 3c. On the other hand, the morphology can be distinguished between the compact polymeric phase and spherical

SiO_2 grains for PANI/SiO_2 composite, as shown in Figure 3b, and for poly(9ANI-co-1Py)/SiO_2, poly(2ANI-co-1Py)/SiO_2, poly(1ANI-co-2Py)/SiO_2, and poly(1ANI-co-1Py)/SiO_2 samples, in which ANI has a major or comparable amount to Py in the starting monomer ratio, as shown in Figure 3d–g, respectively.

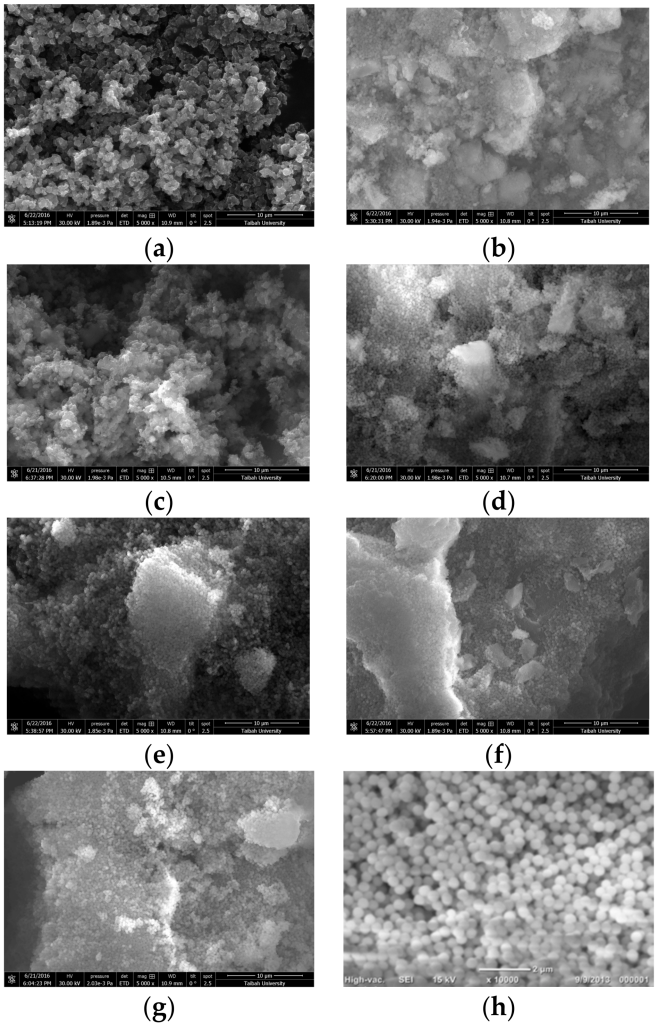

Figure 3. Scanning electron microscope (SEM) images of PPy/SiO_2 (**a**); PANI/SiO_2 (**b**), and different poly(ANI-co-Py) composites in the monomer ratios of 1:9 (**c**); 9:1 (**d**); 1:2 (**e**); 2:1 (**f**); 1:1 (**g**); and silica (**h**).

2.1.3. Thermal Analysis

The thermal behavior of pre-dried homo- and copolymer composites in the temperature range of 200–700 °C, is presented in Figure 4; for PANI/SiO_2 composite, it is shown in Figure 4a. The first stage of degradation, before 400 °C, corresponds to the degradation of low molecular weight polymeric chains. At temperatures above 400 °C, the polymer completely decomposes with a weight loss of 16% [43]. The residual is assigned to SiO_2 which is characterized by its high thermal stability [44]. The poly(9ANI-co-1Py)/SiO_2 and poly(2ANI-co-1Py)/SiO_2 samples offer exactly the same thermal behavior as homo-PANI composite with relatively higher thermal stabilities as indicated by the reduced weight loss values of 15% and 11%, respectively. For PPy/SiO_2 composite, as shown in Figure 4b, the degradation of the polymer chain starts at temperature above 250 °C [45] with a 20% weight loss. An identical TGA curve is assigned to the poly(1ANI-co-9Py)/SiO_2 sample, while very similar behavior with a reduced weight loss of 13% is shown by the poly(1ANI-co-2Py)/SiO_2 sample. The poly(1ANI-co-1Py)/SiO_2 sample, as shown in Figure 4c, shows a combined thermal behavior for

which two degradation steps can be observed, the first at temperature above 250 °C with a weight loss of 2% and the second stage starts above 400 °C with a weight loss of 7%; that is to say, a total polymer percent of 9%. It can be concluded that the copolymerization enhances the thermal stability and this effect is more pronounced by using comparable starting monomer ratios. In other words, the highest thermal stability is assigned to the poly(1ANI-co-1Py)/SiO_2 sample, prepared by using an equal starting monomer ratio.

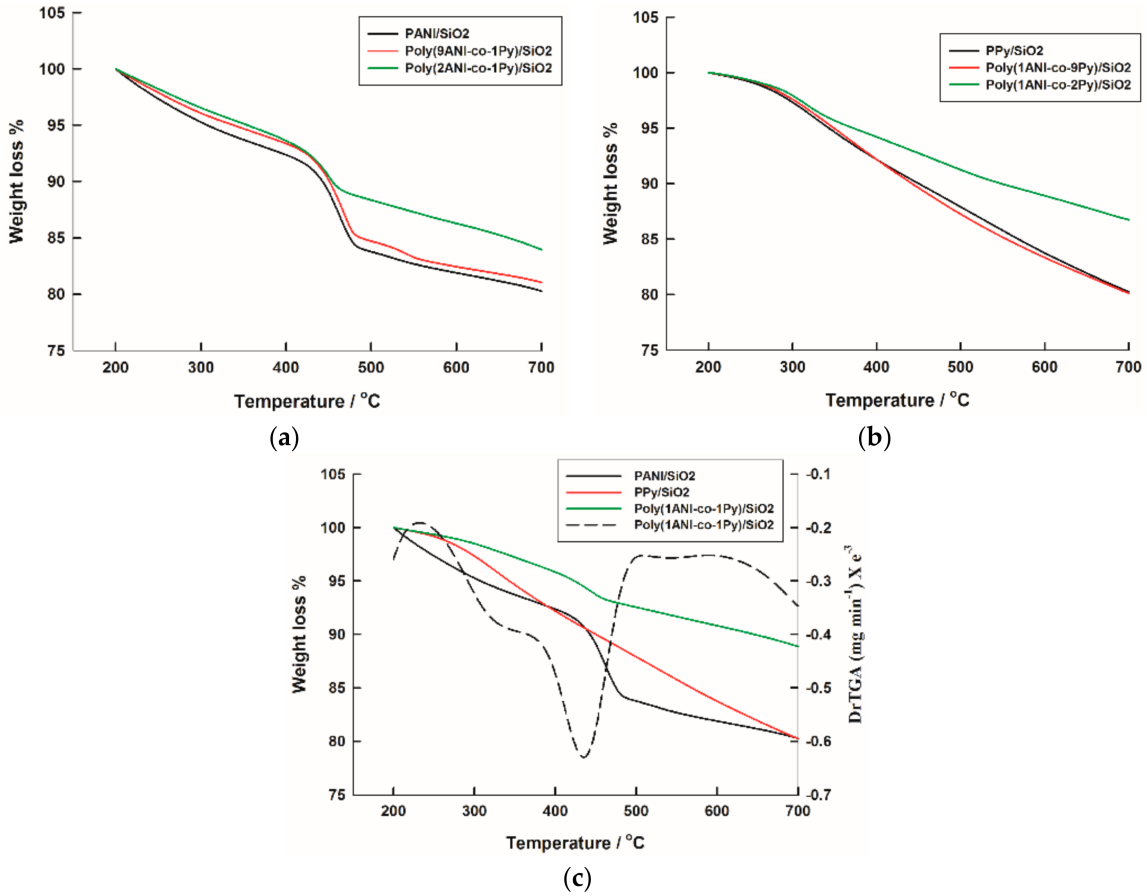

Figure 4. Thermal gravimetric analysis (TGA) curves of (**a**) PANI, poly(9ANI-co-1Py), and poly(2ANI-co-1Py); (**b**) PPy, poly(1ANI-co-9Py), and poly(1ANI-co-2Py); and (**c**) PANI, PPy, and poly(1ANI-co-1Py) composites with SiO_2.

2.1.4. Fourier Transform Infrared Spectroscopy Structural Characterization

Fourier transform infrared spectroscopy (FTIR) spectra of PANI and PPy and their different copolymer composites with SiO_2 are shown in Figure 5. It has been reported that the FTIR spectrum of PANI has peaks at 1558 and 1461 cm^{-1} assigned to the C=N and C=C stretching of quinoid and benzenoid rings, respectively and peaks at 1289 and 824 cm^{-1} for the stretching of C–N and bending of C–H (out of plane) in the benzene ring, respectively [26]. However, the FTIR spectrum of PPy consists of peaks at 1549 and 1460 cm^{-1} assigned to asymmetric and symmetric C–C stretching vibrations of the pyrrole ring, at 1314 cm^{-1} for C–N stretching vibration and at 1050 cm^{-1} for bending vibration of the C–H bond in the pyrrole ring [35]. It can be seen in Figure 5a that PANI/SiO_2, poly(2ANI-co-1Py)/SiO_2, and poly(9ANI-co-1Py)/SiO_2 samples have identical FTIR spectra that contain all the characteristic PANI peaks with a slight shift due to the composite formation with SiO_2; this agrees with the fact that PANI constitutes the major phase in poly(2ANI-co-1Py)/SiO_2, and poly(9ANI-co-1Py)/SiO_2 samples. On the other hand, PPy/SiO_2, poly(1ANI-co-1Py)/SiO_2, poly(1ANI-co-2Py)/SiO_2, and poly(1ANI-co-9Py)/SiO_2 samples have similar FTIR spectra that consist of the PPy characteristic peaks.

In addition, a peak at 1090–1110 cm^{-1} appears in all homo- and copolymer composites; this peak is assigned to Si–O–Si stretching vibrations which ascertains the presence of SiO_2 in all samples [46].

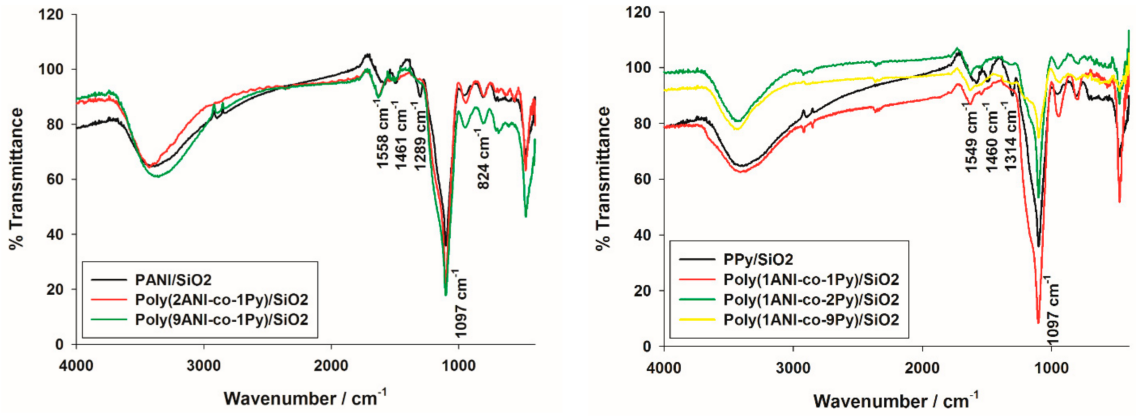

Figure 5. Fourier transform infrared spectroscopy (FTIR) spectra of (**a**) PANI, poly(2ANI-co-1Py), and poly(9ANI-co-1Py); and (**b**) PPy, poly(1ANI-co-1Py), poly(1ANI-co-2Py), and poly(1ANI-co-9Py) composites with SiO_2.

2.2. Nano-Copolymer Composites as Sorbents for CR Removal

In this section, the prepared nano-poly(ANI-co-Py) composites with SiO_2 are employed as sorbents for the removal of CR dye from aqueous solutions. The copolymerization effect on the sorption capacity, with different starting monomer ratios is investigated by performing the adsorption test with different initial dye concentrations ranging from 5 to 100 ppm. Then, proper adsorption isotherm models are tested to analyze the adsorption data.

Langmuir and Fruendlich isotherms are applied to the data of CR adsorption onto different nano-composites. The Langmuir isotherm describes the adsorption of adsorbate on homogeneous adsorbent. It explains the monolayer adsorption where there are no interactions between the adsorbate molecules. The linear equation of the Langmuir model can be represented by [47]:

$$\frac{C_e}{q_e} = \frac{1}{q_m K_L} + \frac{C_e}{q_m} \quad (1)$$

where q_m is the maximum amount sorbed (mg g^{-1}) when the monolayer is complete. K_L is the Langmuir constant which is related to the energy of the adsorption (L mg^{-1}).

For dimensionless constant, R_L can be defined as follows:

$$R_L = \frac{1}{1 + K_L C_i} \quad (2)$$

where K_L is the Langmuir constant, C_i is the initial dye concentration (mg L^{-1}). R_L value indicates that the Langmuir isotherm is favorable ($0 < R_L < 1$), unfavorable ($R_L > 1$), linear ($R_L = 1$) and irreversible ($R_L = 0$) [48].

The Freundlich isotherm describes the adsorption of adsorbate on a heterogeneous adsorbent. The linear equation of the Freundlich model is given as [48]:

$$\ln q_e = \ln K_f + \frac{1}{n} \ln C_e \quad (3)$$

where K_f and n are isotherm constants that indicate the adsorption capacity and intensity of the adsorption, respectively.

Figure 6 shows the Langmuir and Freundlich adsorption isotherms of poly(2ANI-co-1Py) composite with SiO_2 for CR, as an example. Langmuir and Freundlich adsorption parameters for PANI/SiO_2, PPy/SiO_2 and different copolymer composites are calculated and listed in Table 2.

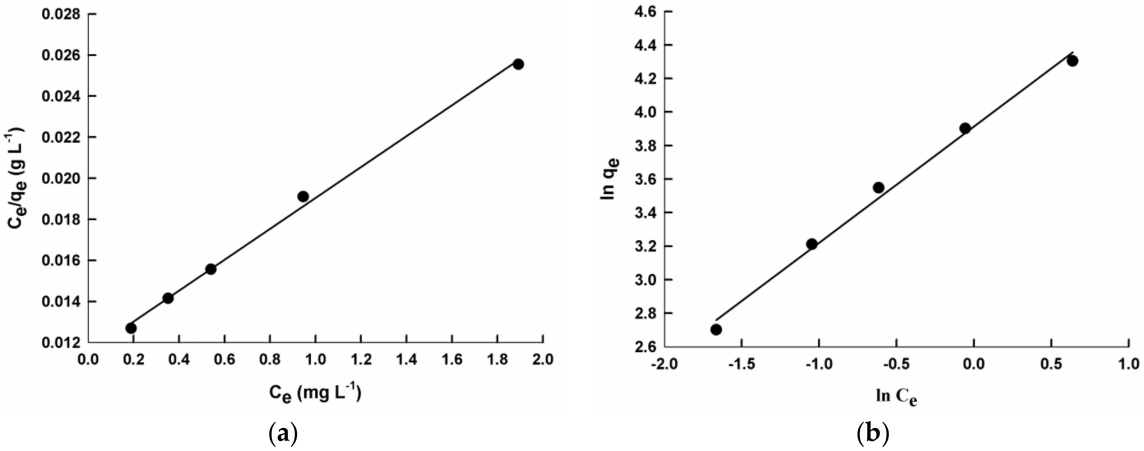

Figure 6. Langmuir (**a**) and Freundlich (**b**) isotherms for Congo red (CR) adsorption onto poly(2ANI-co-1Py)/SiO_2 composite.

Table 2. Adsorption isotherm constants, maximum adsorption capacity (q_m), Langmuir constant (K_L), and Freundlich constants (K_f and n), with correlation coefficient values, r^2, for Congo red (CR) adsorption onto the PANI/SiO_2, PPy/SiO_2 and different copolymer composites.

Langmuir Constants		q_m **(mg g^{-1})**	K_L **(L mg^{-1})**	R_L	r^2
PANI/SiO_2		50.0	0.190	0.05–0.51	0.981
PPy/SiO_2		90.9	0.096	0.09–0.68	0.998
Copolymers/SiO_2 composites					
ANI	Py	q_m **(mg g^{-1})**	K_L **(L/mg)**	R_L	r^2
1	1	83.3	0.285	0.03–0.26	0.986
9	1	62.5	0.592	0.01–0.05	0.999
1	9	83.3	0.260	0.03–0.11	0.996
2	1	142.9	0.636	0.01–0.05	0.997
1	2	41.7	0.235	0.03–0.12	0.998
Freundlich Constants		K_f **(mg$^{1-(1/n)}$L$^{1/n}$/g)**	n	r^2	
PANI/SiO_2		7.2	1.58	0.978	
PPy/SiO_2		7.4	1.21	0.993	
Copolymers/SiO_2 composites					
ANI	Py	K_f **(mg$^{1-(1/n)}$L$^{1/n}$/g)**	n	r^2	
1	1	16.2	1.34	0.970	
9	1	21.8	2.01	0.960	
1	9	18.4	1.98	0.920	
2	1	50.1	1.44	0.992	
1	2	13.4	3.70	0.949	

According to the correlation coefficient values (r^2) of both isotherms, as shown in Table 2, it can be concluded that the Langmuir isotherm fits the adsorption data better than the Freundlich isotherm (r^2 values are closer to unity in the case of the former). Therefore, the adsorption of CR on PANI/SiO_2, PPy/SiO_2, and its different copolymer composites occurs at homogeneous adsorption sites to form the adsorbate monolayer. The maximum adsorption capacity values are calculated and listed in Table 2. It can be seen that PPy/SiO_2 composite has a larger adsorption capacity than that of PANI/SiO_2

composite; q_m values are 90.9 and 50.0 mg g^{-1} which may be due to its larger surface area of 122.8 and 72.4 m^2 g^{-1}, respectively. The copolymerization decreases the sorption efficiency of PPy/SiO_2 composite, except for the poly(2ANI-co-1Py)/SiO_2 sample, the q_m value of which is 142.9 mg g^{-1}. However, the copolymerization increases the sorption efficiency of PANI/SiO_2 composite, except for the poly(1ANI-co-2Py)/SiO_2 sample, the q_m value of which is 41.7 mg g^{-1}. It is worth mentioning that the poly(2AN-co-1Py)/SiO_2 sample has superior sorption capacity compared to the homopolymer and other copolymer composites, the q_m value of which is 142.9 mg g^{-1}. This can be explained by its unique morphology of 1D nano-fibers, which results in enhanced sorption properties [42].

Therefore, the starting monomer ratio, used during the synthesis, affects not only each monomer composition in the copolymer but also the copolymer surface area, and morphology, as well as the polymeric phase amount in the composite, as indicated by the TGA results. All these effects mean that the starting monomer ratio is an important factor in the evaluation of the sorption ability of the copolymer composite.

3. Materials and Methods

3.1. Chemicals

Tetraethylorthosilicate, ANI (99.5%), Py (98%), ferric chloride, sulfuric acid (95–97%), absolute ethanol (99.8%), ammonium hydroxide (33%), and cetyltrimethylammonium bromide (CTAB) are purchased from Sigma Aldrich. CR ($C_{32}H_{22}N_6Na_2O_6S_2$) was bought from (Brixworth, Northants, UK). All solutions were prepared by double distilled water.

3.2. Preparation of Nano-Silica

Silica nano-particles can be prepared by the hydrolysis of tetraethylorthosilicate in ethanol medium in the presence of ammonium hydroxide based on the method reported by Rao et al. [46]. An amount of 10.8 mL of water is first added into 58 mL of ethanol and stirred for 10 min. An amount of 1.6 mL of tetraethylorthosilicate is then added and again stirred for 20 min. An amount of 2.6 mL ammonium hydroxide is added as a catalyst to promote the condensation reaction. The mixture is stirred for 1 h to obtain a white turbid SiO_2 solution.

3.3. Preparation of Nano-Copolymer Composites

Nano-copolymer composites have been chemically prepared by the oxidative copolymerization of ANI and Py in sulfuric acid as a dopant in the presence of nano-silica particles dispersion. Nano-silica is first dispersed in 10^{-3} mol L^{-1} CTAB solution and sonicated for 30 min. Then, $FeCl_3$ dissolved in distilled water is added. While stirring, 0.1 mol L^{-1} of ANI and Py solutions dissolved in 0.1 mol L^{-1} H_2SO_4, in different mixed volume ratios—(ANI:Py) 1:1, 1:2, 2:1, 9:1, 1:9—are injected into the solution drop by drop. The ratio of nano-silica/monomers/$FeCl_3$ is 1:2:2. After 6 h, nano-composites are filtered and washed several times with distilled water, then placed in an 80 °C oven until dry. CTAB enhances the solubility of Py and improves the adsorption capacity of composites [31].

3.4. Adsorption Experiment

CR dye solutions used in adsorption experiments are prepared by diluting the stock solution (1000 mg L^{-1}) to required concentrations. The removal of CR by different composites is carried out by adding 0.05 g of the composite into 25 mL of CR solution at pH = 6 (pH meter HI 2210, Hanna instrument, Hanoi, Romania). Then, samples are placed into a shaker water bath (DKZ Series shaking water bath, Shanghai, China) at a constant speed of 135 rpm at room temperature for 24 h. Samples are centrifuged (HeraeusLabfuge200centrifuge, Thermo scientific, Darmstadt, Germany) at 3500 rpm for 1 h. Residual CR concentration is analyzed by using a UV-Vis spectrometer (Evolution 300 UV-VIS, Thermo scientific, London, UK) at λ_{ma} = 498 nm. The percentage of the dye removal can be calculated according to:

$$\text{Removal } \% = \frac{C_0 - C_e}{C_0} \times 100 \quad (4)$$

The amount of CR adsorbed at the equilibrium, q_e (mg g^{-1}) on synthesized nano-composites, is calculated by:

$$q_e = \frac{(C_0 - C_e)V}{W} \quad (5)$$

where C_0 is the initial dye concentration of (mg L^{-1}) and C_e is the equilibrium dye concentration (mg L^{-1}); V is the volume of the solution (L) and W is the mass of the adsorbent (g).

3.5. Characterizations of Nano-Composites

The phase identification of nano-composites is carried out by using X-ray diffractograms (XRD, Shimadzu, XRD-7000, Tokyo, Japan) at 40 kV and 30 mA, using a CuK_α incident beam (λ = 0.154 nm); the scanning range of 2θ is set between 20 and 80 degrees.

The surface morphology of nano-samples is observed by using scanning electron microscopy (SEM, Superscan SS-550, Shimadzu, Tokyo, Japan) and transmission electron microscopy (TEM, JEM 1400, JEOL, Peabody, MA, USA).

The functional groups of nano-composites are identified by Fourier transform infrared spectroscopy (FTIR, IRAffinity-1S, Shimadzu, Tokyo, Japan). TGA is performed after sample drying at 100 °C by using Q600 T.A. Instruments under N_2 atmosphere at a heating rate of 10 °C min^{-1} to investigate the thermal stability of samples.

4. Conclusions

- Nano-conducting copolymer composites of ANI and Py with SiO_2 have been successively prepared with different starting monomer ratios by the chemical oxidation method in the presence of CTAB.
- PANI is the major phase in PANI/SiO_2, and in poly(2ANI-co-1Py)/SiO_2 and poly(9ANI-co-1Py)/SiO_2 samples; PPy is the major phase in PPy/SiO_2, and in poly(1ANI-co-1Py)/SiO_2, poly(1ANI-co-2Py)/SiO_2, and poly(1ANI-co-9Py)/SiO_2 samples.
- Copolymerization decreases surface area values and increases the thermal stability as compared with homopolymer composites, PANI/SiO_2 and PPy/SiO_2.
- Cauliflower shaped morphology can be observed for PPy/SiO_2, poly(1ANI-co-9Py)/SiO_2, poly(1ANI-co-2Py)/SiO_2, and poly(1ANI-co-1Py)/SiO_2 samples. On the other hand, hexagonal-shaped particles are assigned to PANI/SiO_2 and poly(9ANI-co-1Py)/SiO_2 samples. The poly(2ANI-co-1Py)/SiO_2 sample offers unique 1D nano-fibers.
- Copolymerization decreases the sorption efficiency of PPy/SiO_2 composite, except for the poly(2ANI-co-1Py)/SiO_2 sample; it increases the sorption efficiency of PANI/SiO_2 composite, except for the poly(1ANI-co-2Py)/SiO_2 sample. The poly(2AN-co-1Py)/SiO_2 sample has superior sorption capacity compared to homopolymer and other copolymer composites; the q_m value is 142.9 mg g^{-1} due to its unique morphology which results in enhanced sorption properties.

Acknowledgments: Authors extend gratitude and thanks to the King Abdulaziz City for Science and Technology for research funding.

Author Contributions: S.M.A. and K.M.E. conceived and designed the experiments; A.L.L.A.-O. performed the experiments; S.M.A. and A.L.L.A.-O. analyzed the data; K.M.E. and A.L.L.A.-O. contributed reagents/materials/analysis tools; S.M.A. and A.L.L.A.-O. wrote the paper.

Conflicts of Interest: The founding sponsors had no role in the design of the study; in the collection, analyses, or interpretation of data; in the writing of the manuscript, and in the decision to publish the results.

References

1. Kumar, R.; Singh, S.; Yadav, B.C. Conducting polymers: Synthesis, properties and applications. *Int. Adv. Res. J. Sci. Eng. Technol.* **2015**, *2*, 110–124.
2. Strumpler, R.; Glatz-Reichenbach, J. Conducting polymer composites. *J. Electroceram.* **1999**, *3*, 329–346. [CrossRef]
3. Chaudhary, V.; Kaur, A. Enhanced and selective ammonia sensing behaviour of poly(aniline-co-pyrrole) nanospheres chemically oxidative polymerized at low temperature. *J. Ind. Eng. Chem.* **2015**, *26*, 143–148. [CrossRef]
4. Durairaj, S.; Vaithilingam, S. Hydrothermal assisted synthesis of zeolite based nickel deposited poly(pyrrole-co-fluoro aniline)/CuS catalyst for methanol and sulphur fuel cell applications. *J. Electroanal. Chem.* **2017**, *787*, 55–65. [CrossRef]
5. Qiu, L.; Zhang, S.; Zhanga, L.; Suna, M.; Wang, W. Preparation and enhanced electrochemical properties of nano-sulfur/poly(pyrrole-co-aniline) cathode material for lithium/sulfur batteries. *Electrochim. Acta* **2010**, *55*, 4632–4636. [CrossRef]
6. Liang, B.; Qin, Z.; Li, T.; Dou, Z.; Zeng, F.; Cai, Y.; Zhu, M.; Zhou, Z. Poly(aniline-co-pyrrole) on the surface of reduced graphene oxide as high-performance electrode materials for supercapacitors. *Electrochim. Acta* **2015**, *177*, 335–342. [CrossRef]
7. Dhibar, S.; Bhattacharya, P.; Hatui, G.; Das, C.K. Transition metal doped poly(aniline-co-pyrrole)/multi-walled carbon nanotubes nanocomposite for high performance supercapacitor electrode materials. *J. Alloys Compd.* **2015**, *625*, 64–75. [CrossRef]
8. Govindarajua, K.M.; Prakash, V.C.A. Synthesis of zinc modified poly(aniline-co-pyrrole) coatings and its anti-corrosive performance on low nickel stainless steel. *Colloids Surf. A Physicochem. Eng. Asp.* **2015**, *465*, 11–19. [CrossRef]
9. Bhaumik, M.; McCrindle, R.; Maity, A. Efficient removal of congo red from aqueous solutions by adsorption onto interconnected polypyrrole–polyaniline nanofibres. *Chem. Eng. J.* **2013**, *228*, 506–515. [CrossRef]
10. Bhaumik, M.; Maity, A.; Srinivasu, V.V.; Onyango, M.S. Removal of hexavalent chromium from aqueous solution using polypyrrole–polyaniline nanofibers. *Chem. Eng. J.* **2012**, *181–182*, 323–333. [CrossRef]
11. Afkhami, A.; Moosavi, R. Adsorptive removal of Congo red a carcinogenic textile dye from aqueous solutions by maghemite nanoparticles. *J. Hazard. Mater.* **2010**, *174*, 398–403. [CrossRef] [PubMed]
12. Unnithan, M.R.; Anirudhan, T.S. The kinetics and thermodynamics of sorption of Cr(VI) onto the iron(III) complex of a carboxylated polymer acrylamide-grafted sawdust. *Ind. Eng. Chem. Res.* **2001**, *40*, 2693–2701. [CrossRef]
13. Chatterjee, S.; Lee, D.S.; Lee, M.W.; Woo, S.H. Enhanced adsorption of Congo red from aqueous solutions by chitosan hydrogel beads impregnated with cetyltrimethyl ammonium bromide. *Bioresour. Technol.* **2009**, *100*, 2803–2809. [CrossRef] [PubMed]
14. Han, R.; Ding, D.; Xu, Y.; Zou, W.; Wang, Y.; Li, Y.; Zou, L. Use of rice husk for adsorption of congo red from aqueous solution in column mode. *Bioresour. Technol.* **2008**, *99*, 2938–2946. [CrossRef] [PubMed]
15. Reddy, M.C.; Sivaramakrishna, L.; Reddy, A.V. The use of an agricultural waste material, Jujuba seeds for the removal of anionic dye (congo red) from aqueous medium. *J. Hazard. Mater.* **2012**, *203–204*, 118–127. [CrossRef] [PubMed]
16. Mittal, A.; Mittal, J.; Malviya, A.; Gupta, V.K. Adsorptive removal of hazardous anionic dye "congo red" from wastewater using waste materials and recovery by desorption. *J. Colloid Interface Sci.* **2009**, *340*, 16–26. [CrossRef] [PubMed]
17. Mall, I.D.; Srivastava, V.C.; Agarwal, N.K.; Mishra, I.M. Removal of congo red from aqueous solution by bagasse fly ash and activated carbon: Kinetic study and equilibrium isotherm analyses. *Chemosphere* **2005**, *61*, 492–501. [CrossRef] [PubMed]
18. Tor, A.; Cengeloglu, Y. Removal of congo red from aqueous solution by adsorption onto acid activated red mud. *J. Hazard. Mater.* **2006**, *138*, 409–415. [CrossRef] [PubMed]
19. Chowdhury, A.N.; Jesmeen, S.R.; Hossain, M.M. Removal of dyes from water by conducting polymeric adsorbent. *Polym. Adv. Technol.* **2004**, *15*, 633–638. [CrossRef]
20. Mahanta, D.; Madras, G.; Radhakrishnan, S.; Patil, S. Adsorption of sulfonated dyes by polyaniline emeraldine salt and its kinetics. *J. Phys. Chem. B* **2008**, *112*, 10153–10157. [CrossRef] [PubMed]

21. Ayad, M.M.; Abu El-Nasr, A.; Stejskal, J. Kinetics and isotherm studies of methylene blue adsorption onto polyaniline nanotubes base/silica composite. *J. Ind. Eng. Chem.* **2012**, *18*, 1964–1969. [CrossRef]
22. Yao, W.; Shen, C.; Lu, Y. Fe_3O_4/C/polyaniline trilaminar core–shell composite microspheres as separable adsorbent for organic dye. *Compos. Sci. Technol.* **2013**, *87*, 8–13. [CrossRef]
23. Jebreil, S.A. Removal of tartrazine dye form aqueous solutions by adsorption on the surface of polyaniline/iron oxide composite. *Int. Sch. Sci. Res. Innov.* **2014**, *8*, 1346–1351.
24. Patil, M.R.; Shrivastava, V.S. Adsorption removal of carcinogenic acid violet19 dye from aqueous solution by polyaniline-Fe_2O_3 magnetic nano-composite. *J. Mater. Environ. Sci.* **2015**, *6*, 11–21.
25. Patil, M.R.; Shrivastava, V.S. Adsorption of malachite green by polyaniline–nickel ferrite magnetic nanocomposite: An isotherm and kinetic study. *Appl. Nanosci.* **2014**, *5*, 809–816. [CrossRef]
26. Khairy, M. Polyaniline-$Zn_{0.2}Mn_{0.8}Fe_2O_4$ ferrite core-shell composite: Preparation, characterization and properties. *J. Alloys Compd.* **2014**, *608*, 283–291. [CrossRef]
27. Javadian, H.; Angaji, M.T.; Naushad, M. Synthesis and characterization of polyaniline/γ-alumina nanocomposite: A comparative study for the adsorption of three different anionic dyes. *J. Ind. Eng. Chem.* **2014**, *20*, 3890–3900. [CrossRef]
28. Dhanavel, S.; Nivethaa, E.A.K.; Dhanapal, K.; Gupta, V.K.; Narayanan, V.; Stephen, A. α-MoO_3/polyaniline composite for effective scavenging of rhodamine B, congo red and textile dye effluent. *RSC Adv.* **2016**, *6*, 28871–28886. [CrossRef]
29. Bhaumik, M.; Mccrindle, R.I.; Maity, A. Enhanced adsorptive degradation of congo red in aqueous solutions using polyaniline/Fe composite nanofibers. *Chem. Eng. J.* **2015**, *260*, 716–729. [CrossRef]
30. Janaki, V.; Vijayaraghavan, K.; Oh, B.; Lee, K.; Muthuchelian, K.; Ramasamy, A.K.; Kamala-Kannan, S. Starch/polyaniline nanocomposite for enhanced removal of reactive dyes from synthetic effluent. *Carbohydr. Polym.* **2012**, *90*, 1437–1444. [CrossRef] [PubMed]
31. Ahmed, S.M.; El-Dib, F.I.; El-Gendy, N.S.; Sayed, W.M. Kinetic study for the removal of anionic sulphonated dye from aqueous solution using nano-polyaniline and Baker' s yeast. *Arab. J. Chem.* **2012**, *9*, S1721–S1728. [CrossRef]
32. Li, J.; Feng, J.; Yan, W. Excellent adsorption and desorption characteristics of polypyrrole/TiO_2 composite for methylene Blue. *Appl. Surf. Sci.* **2013**, *279*, 400–408. [CrossRef]
33. Li, J.; Zhang, Q.; Feng, J.; Yan, W. Synthesis of PPy-modified TiO_2 composite in H_2SO_4 solution and its novel adsorption characteristics for organic dyes. *Chem. Eng. J.* **2013**, *225*, 766–775. [CrossRef]
34. Bagher, M.; Yamini, Y.; Dayeni, M.; Seidi, S. Adsorptive removal of alizarin red-S and alizarin yellow GG from aqueous solutions using polypyrrole-coated magnetic nanoparticles. *Biochem. Pharmacol.* **2015**, *3*, 529–540.
35. Shanehsaz, M.; Seidi, S.; Ghorbani, Y.; Shoja, S.M.R.; Rouhani, S. Polypyrrole-coated magnetic nanoparticles as an efficient adsorbent for RB19 synthetic textile dye: Removal and kinetic study. *Spectrochim. Acta Part A Mol. Biomol. Spectrosc.* **2015**, *149*, 481–486. [CrossRef] [PubMed]
36. Ali, S.M.; Emran, K.M.; Al-Oufi, A.L.L. Adsorption of organic pollutants by nano-conducting polymers composites: Effect of the supporting nano-oxide type. *J. Mol. Liq.* **2017**, *233*, 89–99. [CrossRef]
37. Nittaya, T.; Apinon, N. Synthesis and characterization of nanosilica from rice husk ash prepared by precipitation method. *Nat. Sci.* **2008**, *7*, 59–65.
38. Schnitzler, D.C.; Zarbin, A.J.G. Organic/Inorganic hybrid materials formed from TiO_2 nanoparticles and polyaniline. *J. Braz. Chem. Soc.* **2004**, *15*, 378–384. [CrossRef]
39. Wei, F.; Enhai, S.; Akihiko, F.; Hongcai, W.; Koichi, N.; Katsumi, Y. Synthesis and characterization of photoconducting polyaniline-TiO_2 nanocomposite. *Bull. Chem. Soc. Jpn.* **2000**, *73*, 2627–2633.
40. Partch, R.; Gangolli, S.G.; Matijevic, E.; Cai, W.; Arajst, S. Conducting polymer composites: Surface-induced polymerization of pyrrole on iron (111) and cerium(IV) oxide particles. *J. Colloid Interface Sci.* **1991**, *144*, 27–35. [CrossRef]
41. Su, N.; Li, H.B.; Yuan, S.J.; Yi, S.P.; Yin, E.Q. Synthesis and characterization of polypyrrole doped with anionic spherical polyelectrolyte brushes. *Express Polym. Lett.* **2012**, *6*, 697–705. [CrossRef]
42. Li, D.; Huang, J.; Kaner, R.B. Polyaniline nanofibers: A unique polymer nanostructure for versatile applications. *Acc. Chem. Res.* **2009**, *42*, 135–145. [CrossRef] [PubMed]

43. Ansari, S.A.; Parveen, N.; Han, H.; Ansari, O. Fibrous polyaniline/manganese oxide nanocomposites as supercapacitor electrode materials and cathode catalysts for improved power production in microbial fuel cells. *Phys. Chem. Chem. Phys.* **2016**, *18*, 9053–9060. [CrossRef] [PubMed]
44. Kumar, S.A.; Bhandari, H.; Sharma, C.; Khatoon, F.; Dhawan, S.K. A new smart coating of polyaniline-SiO_2 composite for protection of mild steel against corrosion in strong acidic medium. *Polym. Int.* **2013**, *62*, 1192–1201. [CrossRef]
45. Bose, S.; Kuila, T.; Uddin, M.E.; Kim, N.H.; Lau, A.K.T.; Lee, J.H. In-situ synthesis and characterization of electrically conductive polypyrrole/graphene nanocomposites. *Polymer* **2010**, *51*, 5921–5928. [CrossRef]
46. Rao, K.S.; El-Hami, K.; Kodaki, T.; Matsushige, K.; Makino, K. A novel method for synthesis of silica nanoparticles. *J. Colloid Interface Sci.* **2005**, *289*, 125–131. [CrossRef] [PubMed]
47. Du, Q.; Sun, J.; Li, Y.; Yang, X.; Wang, X.; Wang, Z.; Xia, L. Highly enhanced adsorption of congo red onto graphene oxide/chitosan fibers by wet-chemical etching off silica nanoparticles. *Chem. Eng. J.* **2014**, *245*, 99–106. [CrossRef]
48. Dawood, S.; Sen, T.K. Removal of anionic dye congo red from aqueous solution by raw pine and acid-treated pine cone powder as adsorbent: Equilibrium, thermodynamic, kinetics, mechanism and process design. *Water Res.* **2012**, *46*, 1933–1946. [CrossRef] [PubMed]

Sample Availability: Samples of nano-conducting copolymer composites, poly(ANI-co-Py)/SiO_2, with different monomeric ratio, are available from the authors.